

Organic & Biomolecular Chemistry

Accepted Manuscript



This is an *Accepted Manuscript*, which has been through the Royal Society of Chemistry peer review process and has been accepted for publication.

Accepted Manuscripts are published online shortly after acceptance, before technical editing, formatting and proof reading. Using this free service, authors can make their results available to the community, in citable form, before we publish the edited article. We will replace this *Accepted Manuscript* with the edited and formatted *Advance Article* as soon as it is available.

You can find more information about *Accepted Manuscripts* in the [Information for Authors](#).

Please note that technical editing may introduce minor changes to the text and/or graphics, which may alter content. The journal's standard [Terms & Conditions](#) and the [Ethical guidelines](#) still apply. In no event shall the Royal Society of Chemistry be held responsible for any errors or omissions in this *Accepted Manuscript* or any consequences arising from the use of any information it contains.

Design, synthesis and initial characterisation of a radiolabelled [^{18}F]pyrimidoindolone probe for detecting activated caspase-3/7

Cite this: DOI: 10.1039/x0xx00000x

Received 00th January 2012,
Accepted 00th January 2012

DOI: 10.1039/x0xx00000x

www.rsc.org/

A. Udemba,^a G. Smith,^b Q-D. Nguyen,^c M. Kaliszczak,^a L. Carroll,^a R. Fortt,^d M. J. Fuchter^c and E. O. Aboagye^{a*}

Evasion of apoptosis is one of the six initially proposed hallmarks of cancer, and as such, a method to detect apoptosis in a tumour would be of considerable interest in both clinical trials of new cancer therapeutics, as well as for routine patient management. Activation of caspase-3/7 is a key biomarker of cellular apoptosis. Herein we describe the design, synthesis and initial characterisation of the first pyrimidoindolone compound for detection of caspase-3/7 activation using positron emission tomography.

Introduction

Evasion of apoptosis is one of the six initial hallmarks of cancer identified by Hanahan and Weinberg, and many chemotherapeutics, together with radiotherapy approaches, actively induce apoptosis as a treatment strategy.^[1] A method to quantitatively assess the degree of apoptosis in a tumour would therefore be of considerable interest in both clinical trials of new therapeutic strategies and in routine patient management. Conventional approaches to quantifying response to treatment, based on the Response Evaluation Criteria in Solid Tumors (RECIST) guidelines using anatomical imaging, are of limited utility for early assessment of response to molecularly targeted cancer therapeutics since tumour size changes typically take many weeks to manifest.^[2] Therefore, a clinically viable strategy to non-invasively annotate the induction of apoptosis is urgently needed. Positron emission tomography (PET) is a minimally invasive imaging technique for quantitative interrogation of biological processes such as cell death.^[3] Probes for PET imaging of cell death targeting phosphatidylserine externalisation (annexin V peptide), membrane permeabilisation ([^{18}F]ML-10) and activated caspase-3 ([^{18}F]WC-IV-3) have attracted interest over recent years.^[4] Caspase-3 has been recognized as the key executioner enzyme that processes critical structural proteins as part of the cascade of cellular demolition, and cleaves additional proteins engaged in the apoptotic

pathway into their active forms (for example, PARP).^[5] Furthermore, conversion of caspase-3 into its active form is the first irreversible step in the apoptotic cascade. As a result of this, caspase-3 represents an attractive target for imaging early apoptosis. Together with other research groups, we have a longstanding interest in imaging caspase-3/7 activity as a biomarker of apoptosis using radiolabelled isatin-5-sulfonamide-based caspase-3/7 inhibitors.^[6] In our case we have evaluated a lead probe, [^{18}F]ICMT-11 (Figure 1), in clinically relevant models of treatment response and we have recently completed a First in Man clinical trial.^[7]

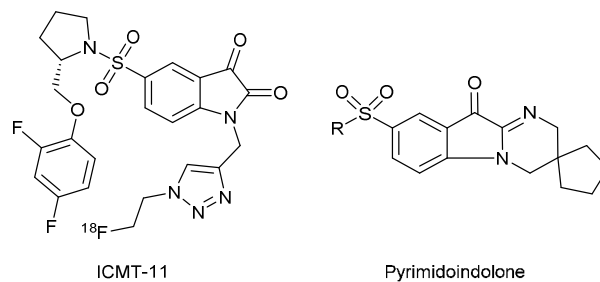


Figure 1 – Structure of the isatin-5-sulfonamide, ICMT-11, and pyrimidoindolone core

Improvement of probe specificity by reduction of non-specific binding was considered a prerequisite for a second-generation caspase-3 targeted agent. We reasoned that this could be achieved by tuning the reactivity of the key C-3 “warhead” β -keto carbonyl, which forms a reversible covalent bond (a thiohemiketal) in the caspase-3 active site, through reaction with an active site cysteine residue. Reduction in the reactivity of this key functionality could potentially reduce non-specific reactions with other thiol-containing residues, such as glutathione, hypothesised to be one of the main reasons for suboptimal signal-to-noise ratios for [^{18}F]ICMT-11. Such alterations to the reactivity of the key warhead carbonyl should not

have a deleterious effect on the formation of the active site thiohemiketal however, since the enzyme-inhibitor complex facilitates thiohemiketal formation. Accordingly, we were attracted to the pyrimidoindolone (Figure 1) class of caspase-3/7 inhibitors.^[8] The pyrimidoindolone scaffold retains a similar selectivity profile in comparison to isatin-based structures, with their mechanism of target interaction involving a two-site binding mode in the same place to that of isatins.^[9] The pyrimidoindolone class of inhibitors has a theoretical advantage compared to the isatin series however, due to the stoichiometry of binding: Pyrimidoindolones have an equal affinity for both active sites of the caspase-3 heterodimer, an attribute not embodied in ICMT-11.^[9] This last observation was of considerable interest, since it immediately doubles the number of potential binding sites offered by the transiently expressed caspase-3 enzyme. Therefore, our aim within this project was the design, synthesis and evaluation of radio-labelled pyrimidoindolone caspase-3 inhibitors, as potential second generation apoptosis imaging agents.

Results and discussion

Rational design of a radiolabelled pyrimidoindolone probe was approached in the following manner. Firstly, the probe required an easily radiolabelled functionality that did not compromise caspase-3 binding affinity or selectivity. To achieve this, we decided to use a copper-catalysed 1,3-dipolar cycloaddition, more routinely known under the umbrella of 'click' chemistry. We have previously observed that this 1,2,3 triazole ring does not impair the high affinity binding to caspase-3/7 in the analogous isatin series.^[6d] As high specific activity is key for caspase imaging, given the low and transient expression of activated caspase-3/7, utilising 'click' chemistry should also allow for a corresponding direct one-step S_N2 labelling methodology to be utilised instead, should complications arise from the radiolabelling strategy. The second design consideration that guided our thinking was the observation that certain compounds within the pyrimidoindolone compound class have poor aqueous stability. To overcome this limitation, we employed a spirocyclic pentane on the imidine ring of the pyrimidoindolone to give **10** (Figure 2) as our target probe structure; known to be more stable under aqueous conditions.^[8]

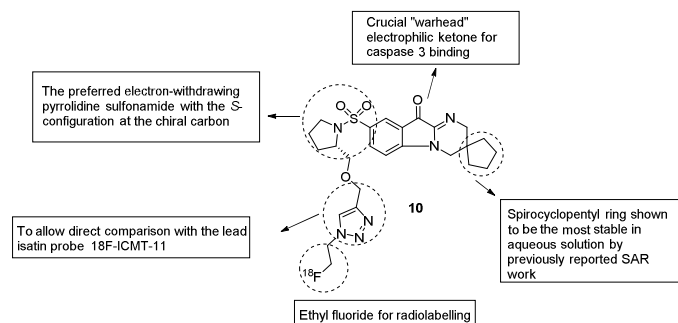
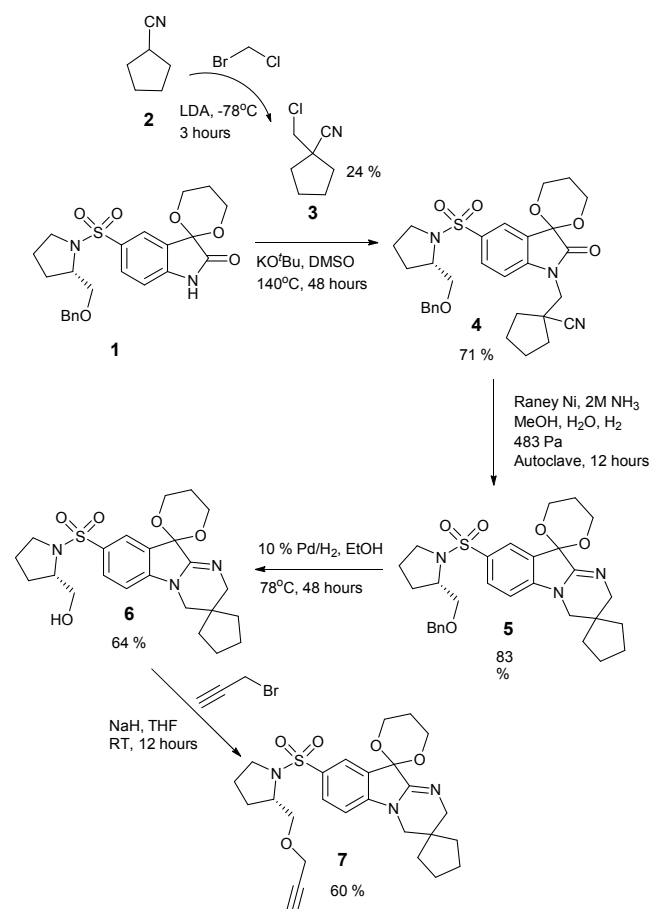


Figure 2- Structure of pyrimidoindolone target highlighting key design features

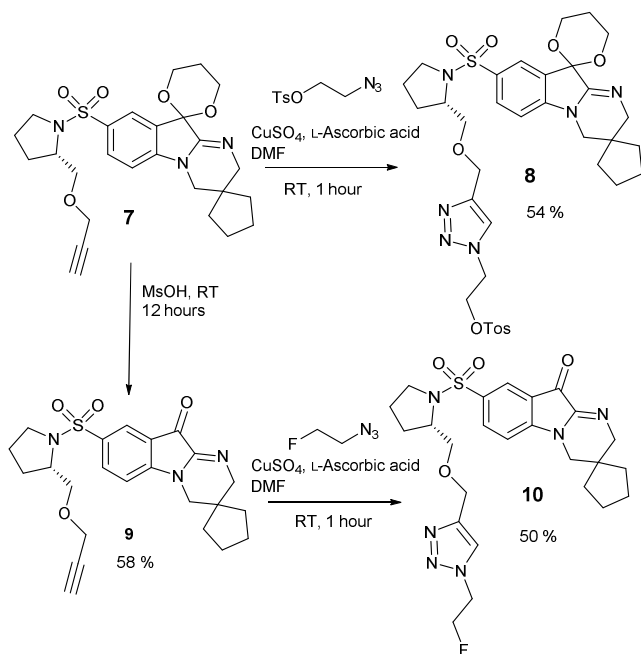
Our route to achieving the synthesis of the pyrimidoindolone core structure **10** is summarised in Scheme 1, starting from the acetal-protected isatin **1**.^[8] Alkylation of isatin **1** at the indole nitrogen with the relevant halogenocyclopentane carbonitrile, followed by cyclocondensation gave the central pyrimidoindolone core structure. The previously reported procedure for synthesis of chloromethylcyclopentanecarbonitrile **3** proved difficult to replicate.^[10] We reasoned that this was the result of instability in the carbanion formed by lithium diisopropylamide-mediated deprotonation of carbonitrile **2**. To overcome this difficulty the cyclopentanecarbonitrile was pre-cooled to -78 °C in the presence of bromochloromethane prior to addition of a cooled (to -78 °C) solution of LDA to give the desired chloromethylcyclopentanecarbonitrile **3** in an acceptable 24 % yield.

Alkylation of isatin **1** with carbonitrile **3** was carried out under basic conditions over 48 hours to afford the desired product in good yield (71 %). Subsequent reduction of the nitrile with a wet Raney nickel/hydrogen mixture and cyclisation of the amine afforded the pyrimidoindolone core **5** directly in good yield (83%), with the mild conditions for the cyclisation reaction likely the result of a Thorpe-Ingold effect from the spiro-substituted cyclopentane ring. The benzyl ether was deprotected using palladium on carbon and the resulting alcohol was alkylated with propargyl bromide to give alkyne **7** ready for radiolabelling studies.



Scheme 1 – Synthetic sequence to form protected pyrimidoindolone alkyne **7**

Reaction of alkyne **7** with tosyl ethyl azide, under standard copper-catalysed conditions, gave the click chemistry product **8** (54 % yield), suitable for radiolabelling by direct [¹⁸F]fluoride displacement, followed by acetal deprotection. Simultaneously alkyne **7** was deprotected to give the click radiolabelling precursor **9**, which could also be reacted with 2-fluoroethyl azide to afford a ‘cold’ standard of the lead pyrimidoindolone structure **10** in moderate yield (50 %).



Scheme 2 – Synthesis of radiochemical precursors **8** and **9**

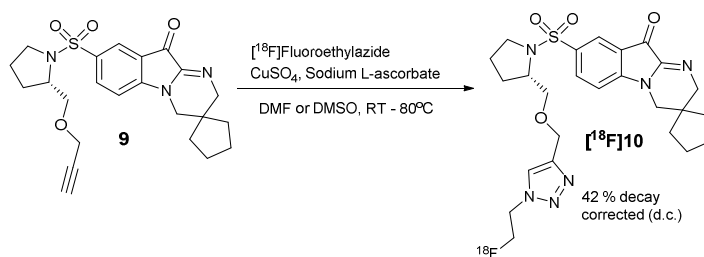
Pyrimidoindolone **10** and ICMT-11 were evaluated in a standard caspase-3 fluorogenic enzyme competition assay, with regular sampling over 90 minutes of incubation. The results are summarised in Table 1, together with corresponding results from the same assay in which caspase-3 was replaced by caspase-8, as a measure of selectivity. The results confirm the caspase-3 selectivity for both inhibitors, and that ICMT-11 has ~16-fold higher affinity for caspase-3 relative to pyrimidoindolone **10**. We did not achieve the same sub-nanomolar affinity of ICMT-11 for caspase-3 as reported in a previous report^[6d]; we suggest this is due to batch variability of the enzymes employed.

Table 1 – IC50 Measurements of ICMT-11 and **10** against Caspase-3 and 8

Incubation Time (min)	IC50 Caspase-3 (nM)		IC50 Caspase-8 (nM)	
	Pyrimido 10	ICMT-11	Pyrimido 10	ICMT-11
15	108.9	13.4	>5000	>5000
30	78.2	1.9	>5000	>5000
60	118.8	5.7	>5000	>5000
90	95.8	4.0	>5000	>5000

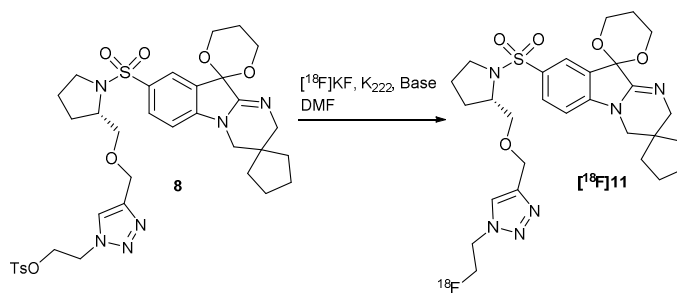
Mean	100.4 ± 8.8	6.3 ± 2.5	-	-
------	-------------	-----------	---	---

We proceeded to investigate ¹⁸F radio-labelling for compound **10**, in order to enable *in vitro* uptake assays to be carried out. The first approach utilised alkyne **9**, in a comparable copper-catalysed alkyne-azide cycloaddition reaction as that carried out previously, only this time employing 2-[¹⁸F]fluoroethyl azide; a strategy successfully employed numerous times within our laboratory on heterocyclic core scaffolds including the analogous isatin compound ICMT-11 (Scheme 3).^{[6d, 11] [12]} However, this click radiolabelling reaction was hampered by a low radiochemical yield and a persistent impurity that co-eluted on semi-preparative HPLC, in a similar manner to that observed for [¹⁸F]ICMT-11.^[6d] This led to re-evaluation of the pyrimidoindolone radiolabelling strategy.



Scheme 3 – Radiolabelling *via* click chemistry to give [¹⁸F]**10**

The direct radiolabelling approach, starting from protected pyrimidoindolone **8** (Scheme 4), was instead investigated.^[13] The first step was to investigate a direct [¹⁸F]fluoride displacement of the tosylate leaving group of precursor **8** under various conditions. The results from HPLC analysis of [¹⁸F]fluoride incorporation from this reaction are summarised in Table 2. Competition was observed between the desired radiolabelling reaction and side reactions, which resulted in the precursor being fully consumed within 10 minutes. Based on our previous experience to radiolabel [¹⁸F]ICMT-11 by the same route, the most significant side reactions are likely base-induced hydrolysis of the tosylate to the corresponding alcohol, and elimination of the tosylate to yield an alkene by-product.^[13] After surveying several options, it became apparent that using a stronger base, such as potassium carbonate, at a higher temperature (110 °C) for 10 minutes gave a radiochemical incorporation (76 %), which was appropriate for further work (entry 10, Table 2).

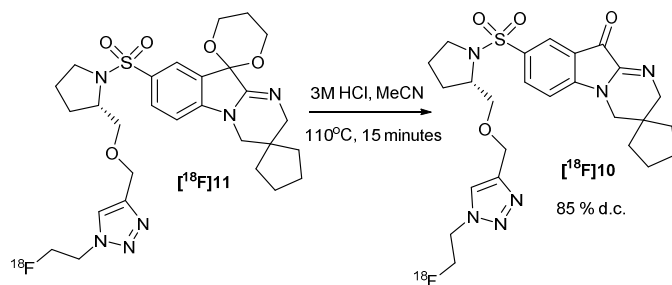


Scheme 4 – Reaction to give protected intermediate [¹⁸F]**11**

Table 2 - Summary of attempted direct displacement reactions to give [¹⁸F]11

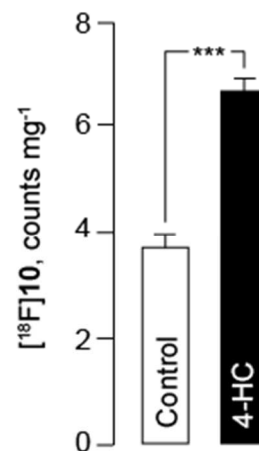
Entry	Time /min	Solvent	Temp (°C)	Base	% ¹⁸ F incorporation*
1	5	DMF	80	K ₂ CO ₃	14
2	10	DMF	80	K ₂ CO ₃	29
3	15	DMF	80	K ₂ CO ₃	30
4	20	DMF	80	K ₂ CO ₃	40
5	5	DMF	110	KHCO ₃	22
6	10	DMF	110	KHCO ₃	26
7	15	DMF	110	KHCO ₃	36
8	20	DMF	110	KHCO ₃	37
9	5	DMF	110	K ₂ CO ₃	63
10	10	DMF	110	K ₂ CO ₃	76
11	10	DMF	110	K ₂ CO ₃	36

With the radiolabelled product [¹⁸F]11 in hand, acetal deprotection was attempted to give the target probe [¹⁸F]10 (Scheme 5). The initially surveyed conditions involved diluting the ¹⁸F⁻ displacement reaction mixture with a 3M HCl solution and heating to 110 °C. Slow and incomplete deprotection was observed, despite further increasing HCl concentration to 5M and the reaction time to 30 minutes. At best, a moderate 50% deprotection was obtained using these conditions. Using H₂SO₄ instead of HCl improved the conversion to the desired [¹⁸F]10, but it proved difficult to neutralise this mixture, in order to allow for preparative HPLC purification; a pH of over 7.4 began to degrade the labelled product. It became apparent that a 3M HCl solution, together with MeCN as a solvent (*via* C18 solid-phase re-formulation of the labelled intermediate [¹⁸F]11) gave vastly improved deprotection (up to 85 % within 15 minutes), whilst maintaining an easier neutralisation process prior to HPLC purification. A decay corrected radiochemical yield of 18 ± 4 % (n = 6) was obtained for the overall two-step synthesis of [¹⁸F]10 from protected tosylate 8.

**Scheme 5** – Optimised deprotection of [¹⁸F]11 to give [¹⁸F]10

Mechanistic determination of caspase-3 selectivity for [¹⁸F]10 in a cell based model of apoptosis was carried out (Figure 3). Radiolabelled [¹⁸F]10 was incubated with 38C13 lymphoma (tumour) cells treated with 4-hydroperoxycyclophosphamide (4-HC), an activated form of cyclophosphamide that induces apoptosis in cells, in direct comparison to previous work carried out with [¹⁸F]ICMT-11.^[14] The results show a significant increase in radioligand uptake after 60 minutes, from around 3.8 counts/mg in control (untreated) cells to 6.4 counts/mg in drug treated cells, an

overall increase in signal of over 60 %. This is in-line with a similar uptake profile seen in [¹⁸F]ICMT-11, which also shows an increase in signal of more than 1.5 times over control uptake. This similarity, despite a noticeable difference in IC₅₀ value for Caspase-3 between [¹⁸F]ICMT-11 and [¹⁸F]10, is probably due to the differences in binding at the active site (single versus dual-binding). Notably overall uptake was lower for [¹⁸F]ICMT-11 when compared to [¹⁸F]10, under identical conditions. Based on our previous experience with [¹⁸F]ICMT-11,^[14] this suggests that [¹⁸F]10 should be a promising compound for caspase-3 imaging.

**Figure 3** - 38C13 lymphoma (tumour) cell uptake of [¹⁸F]10 in untreated control cells (control cells, 0.1% DMSO, 24 h) and 4-hydroperoxycyclophosphamide (4-HC) treated cells (3 μg/mL, 24 h). For all treated and control samples, radioactivity data were expressed as decay-corrected counts per milligram of total cellular protein.

Initial *in vivo* verification of tissue distribution and metabolic stability was carried out, to allow a comparison to the current lead compound [¹⁸F]ICMT-11 (Figure 4). The tissue distribution studies involved intravenous injection of the [¹⁸F]10 into tumour-bearing untreated mice, followed by gamma-counting of relevant organs at 60 minutes post-injection. Similarly to [¹⁸F]ICMT-11 tissue biodistribution profile, high localisation of [¹⁸F]10 activity was seen in the kidney, urine, liver and intestine, suggesting predominantly renal and hepatic elimination, and good clearance from/low distribution to blood/plasma and muscle after 1 hour signifying low background in several other organs; the low bone uptake also suggests minimal defluorination.^{6d}

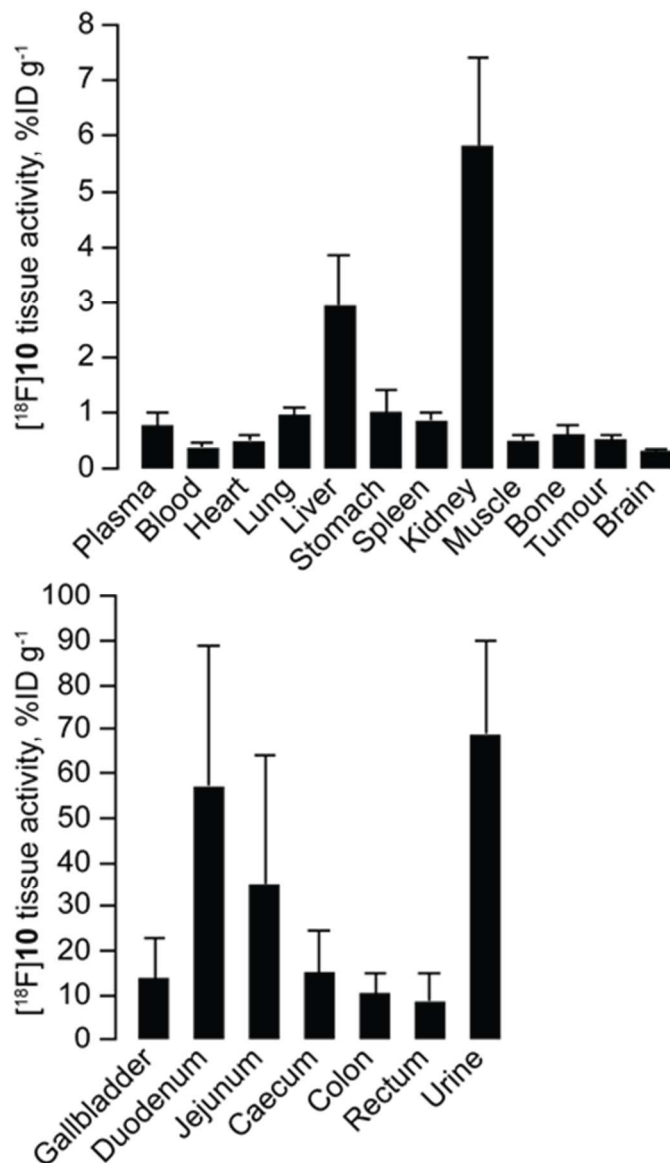


Figure 4: Pyrimidoindolone [¹⁸F]10 biodistribution in mice at 60 min post-injection. Data are mean ± SEM; n = 3 mice

To appreciate why the injected dose in liver and kidney for [¹⁸F]10 appeared to be about ten times higher than that of ICMT-11 at a comparable timepoint, *in vivo* metabolic stability of [¹⁸F]10 was determined in liver, plasma and urine samples (Table 3).^[14] Incubation of [¹⁸F]10 in phosphate buffer solution showed no degradation of the labelled product over 3 hours. Unchanged [¹⁸F]10 was observed in plasma (14%) and in the liver (10%) at 60 min after injection, but at much lower levels to that seen for [¹⁸F]ICMT-11 (65% parent in plasma and 28% in liver). Interestingly, the same metabolite was the dominant peak in all samples at around 4 minutes, again analogous to that of [¹⁸F]ICMT-11, perhaps suggesting a similar metabolite product being formed. In the urine sample, only the unchanged [¹⁸F]10 was observed.

Entry	Metabolite R _t		Parent R _t
	4.5 mins	8.5 mins	10 mins
Plasma	86%	-	14%
Liver	80%	10%	10%
Urine	-	-	100%

Table 3 - *In vivo* metabolism of [¹⁸F]-pyrimidoindolone **10** measured in plasma, liver and urine of mice, with HPLC retention times stated, 60 minutes after injection.

To further evaluate factors that would impact the distribution of [¹⁸F]10 *in vivo*, we tested the transport of the compound across adenocarcinoma Caco-2 monolayers. Non-radiolabelled **10** was incubated at the apical side for 2 hours on a rotating platform and the concentration at the basal side was subsequently measured by HPLC-UV. The rate of membrane transfer was found to be comparable to that of control vinblastine, a cancer drug known to be moderately transported with this assay (Table 4). Additional studies were conducted to verify whether **10** (and therefore [¹⁸F]10) undergoes active efflux by ATP-Binding Cassette (ABC) transporters by measuring bidirectional transport rates. The ratio between secretion (transport from basal to apical side) and absorption (transport from the apical side to basal side) was greater than 3, suggesting that **10** was likely a substrate for ABC transporters (Figure 7).^[15] Treatment with verapamil, an inhibitor of ABC transporter ABCB1 or P-gp, reversed the efflux ratio inferring active efflux. Vinblastine is a known substrate of ABC transporters and similarly, was associated with an efflux ratio greater than 3 that could be reversed by treatment with verapamil.

	Papp A-B (x10 ⁻⁶ cm/sec)	
	Average	SD
10	11	0.6
ICMT-11	36	2.2
Vinblastine	10	0.4

Table 4 - Transport rate of the compounds across the caco-2 cells from the apical to the basal side during 2 hours incubation. The results are mean of n = 3.

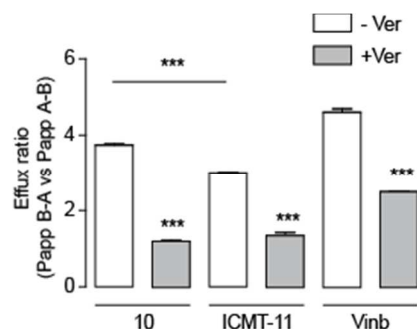


Figure 7 - Efflux ratio in caco-2 transwell assay as expressed by the ratio between the transport from the basal to the apical side (Papp A-B) and the transport from the apical to the basal side (Papp B-A). The results are mean of n = 3. Verapamil was added 1 hour before

incubation with **10** or ICMT-11 at 50 μ M. The results are mean of $n = 3$.

Conclusions

Development of second generation caspase-3 PET imaging probes is required to provide an improved pharmacological profile over that of current gold standard, [18 F]ICMT-11. The pyrimidoindolone core scaffold offers an attractive strategy to achieve this through retention of caspase-3/7 selectivity and nanomolar affinity but potentially reduced propensity to interact with nucleophiles at the key "warhead" carbonyl required for covalent bond formation with a free cysteine thiol in the active site pocket. The chemical synthesis and radiolabelling was achieved *via* both click chemistry and direct S_N2 fluoride displacement, giving a new 18 F-labelled pyrimidoindolone-based compound. The *in vitro* cell uptake assays gave results in line with the previous work using isatins, despite altering the core significantly, and biodistribution was similar to that of [18 F]ICMT-11. Notably, the metabolic profile of [18 F]**10** is almost identical to that of [18 F]ICMT-11. In summary, we report a novel caspase 3 PET imaging agent, [18 F]**10**, which has good *in vitro* selectivity for caspase-3 and promising *in vivo* properties that provide justification for further elucidation of this compounds series. Further optimisation of this compound series will focus on improving metabolic stability and improving caspase-3 affinity. The ultimate goal of research in this compound series remains improvement of the *in vivo* profile, a continuing problem with small-molecule caspase-3 binding radioligands. The widely observed high background uptake in abdominal tissues by this compound class typically limits the potential clinical application to upper torso and peripheral (e.g. head and neck) tumours. The optimal caspase-3 radioligand should have improved clearance from non-target tissue without compromising intracellular transport and caspase-3 binding affinity.

Acknowledgements

We thank CRUK/EPSRC/MRC/DoH (England) for funding (grant C2536/A10337).

Notes and references

^a Comprehensive Cancer Imaging Centre, Department of Surgery and Cancer, Imperial College London, Hammersmith Campus, Du Cane Road, London, W12 0NN.

^b Institute of Cancer Research, 123 Old Brompton Road, London SW7 3RP.

^c Lurie Family Imaging Center, Center for Biomedical Imaging in Oncology, Dana-Farber Cancer Institute, Harvard Medical School, 450 Brookline Avenue, Boston, MA, 02215, USA

^d Division of Imaging Sciences & Biomedical Engineering, King's College London, St Thomas' Hospital, London SE1 7EH.

^e Department of Chemistry, Imperial College London, South Kensington Campus.

Electronic Supplementary Information (ESI) available including NMR characterisation and radiochemical and biological procedures]. See DOI: 10.1039/c000000x/

[1] D. Hanahan and R. A. Weinberg, *Cell*, **2000**, *100*, 57-70.

[2] E. A. Eisenhauer, P. Therasse, J. Bogaerts, L. H. Schwartz, D. Sargent, R. Ford, J. Dancey, S. Arbuck, S. Gwyther, M. Mooney, L. Rubinstein, L. Shankar, L. Dodd, R. Kaplan, D. Lacombe and J. Verweij, *E. J. Cancer* **2009**, *45*, 228-247.

[3] G. Smith, L. Carroll and E. O. Aboagye, *Mol. Imaging Biol.* **2012**, *14*, 653-666.

[4] a) F. G. Blankenberg, P. D. Katsikis, J. F. Tait, R. E. Davis, L. Naumovski, K. Ohtsuki, S. Kopiwoda, M. J. Abrams and H. W. Strauss, *J. Nucl. Med.* **1999**, *40*, 184-191; b) J. Höglund, A. Shirvan, G. Antoni, S.-Å. Gustavsson, B. Långström, A. Ringheim, J. Sörensen, M. Ben-Ami and I. Ziv, *J. Nucl. Med.* **2011**, *52*, 720-725; c) D. L. Chen, D. Zhou, W. Chu, P. E. Herrbrich, L. A. Jones, J. M. Rothfuss, J. T. Engle, M. Geraci, M. J. Welch and R. H. Mach, *Nucl. Med. Biol.* **2009**, *36*, 651-658; d) D. Chen, J. Engle, E. Griffin, J. P. Miller, W. Chu, D. Zhou and R. Mach, *Mol. Imag. Biol.* **2014**, 1-10; e) A. A. Neves and K. M. Brindle, *J. Nucl. Med.* **2014**, *55*, 1-4.

[5] R. C. Taylor, S. P. Cullen and S. J. Martin, *Nature Rev. Mol. Cell Biol.* **2008**, *9*, 231-241.

[6] a) K. Kopka, A. Faust, P. Keul, S. Wagner, H.-J. Breyholz, C. Hoeltke, O. Schober, M. Schaefer and B. Levkau, *J. Med. Chem.* **2006**, *49*, 6704-6715; b) D. Zhou, W. Chu, D. L. Chen, Q. Wang, D. E. Reichert, J. Rothfuss, A. D'Avignon, M. J. Welch and R. H. Mach, *Org. Biomol. Chem.* **2009**, *7*, 1337-1348; c) D. Zhou, W. Chu, J. Rothfuss, C. Zeng, J. Xu, L. Jones, M. J. Welch and R. H. Mach, *Bioorg. Med. Chem. Lett.* **2006**, *16*, 5041-5046; d) G. Smith, M. Glaser, M. Perumal, Q.-D. Nguyen, B. Shan, E. Arstad and E. O. Aboagye, *J. Med. Chem.* **2008**, *51*, 8057-8067.

[7] A. Challapalli, L. M. Kenny, W. A. Hallett, K. Kozlowski, G. Tomasi, M. Gudi, A. Al-Nahas, R. C. Coombes and E. O. Aboagye, *J. Nucl. Med.* **2013**, *54*, 1551-1556.

[8] L. Havran, D. C. Chong, W. E. Childers, P. J. Dollings, A. Dietrich, B. L. Harrison, V. Marathias, G. Tawa, A. Aulabaugh, R. Cowling, B. Kapoor, W. Xu, L. Mosyak, F. Moy, W.-T. Hum, A. Wood and A. J. Robichaud, *Bioorg. Med. Chem.* **2009**, *17*, 7755-7768.

[9] A. Aulabaugh, B. Kapoor, X. Huang, P. Dollings, W.-T. Hum, A. Banker, A. Wood and G. Ellestad, *Biochem.* **2007**, *46*, 9462-9471.

[10] I. A. Cliffe, R. S. Todd and A. C. White, *Synth. Comm.* **1990**, *20*, 1757-1767.

[11] L. Carroll, T. H. Witney and E. O. Aboagye, *MedChemComm* **2013**, *4*, 653-656.

[12] T. H. Witney, L. Carroll, I. S. Alam, A. Chandrashekran, Q.-D. Nguyen, R. Sala, R. Harris, R. J. DeBerardinis, R. Agarwal and E. O. Aboagye, *Cancer Res.* **2014**, *74*, 1319-1328.

[13] R. Fortt, G. Smith, R. O. Awais, S. K. Luthra and E. O. Aboagye, *Nucl. Med. Biol.* **2012**, *39*, 1000-1005.

[14] Q.-D. Nguyen, G. Smith, M. Glaser, M. Perumal, E. Arstad and E. O. Aboagye, *Proc. Nat. Acad. Sci. USA* **2009**, *106*, 16375-16380.

[15] M. Kaliszczak, H. Patel, S. H. B. Kroll, L. Carroll, G. Smith, S. Delaney, D. A. Heathcote, A. Bondke, M. J. Fuchter, R. C. Coombes, A. G. M. Barrett, S. Ali and E. O. Aboagye, *Br J Cancer* **2013**, *109*, 2356-2367.